HHS Public Access

Author manuscript

Acta Biomater. Author manuscript; available in PMC 2016 November 01.

Published in final edited form as:

Acta Biomater. 2015 November ; 27: 194–204. doi:10.1016/j.actbio.2015.08.039.

Quercetin conjugated Poly (β-Amino Esters) Nanogels for the Treatment of Cellular Oxidative Stress

Prachi Gupta, **Sundar P. Authimoolam**, **J. Zach Hilt**, and **Thomas D. Dziubla**

Department of Chemical and Materials Engineering, University of Kentucky, Lexington, KY, 40506-0046, USA

Abstract

PβAE polymers have emerged as highly promising candidates for biomedical and drug delivery applications owing to their tunable, degradable and pH sensitive properties. These polymeric systems can serve as prodrug carriers for the delivery of bioactive compounds which suffer from poor aqueous solubility, low bioavailability and are biologically unstable, such as the antioxidant, quercetin. Using acrylate functionalized quercetin, it is possible to incorporate the polyphenol into the backbone of the polymer matrix, permitting slow release of the intact molecule which is perfectly timed with the polymer degradation. While formulating these quercetin conjugated PβAE matrix into nanocarriers would allow for multiple delivery routes (oral, intravenous, inhalation etc.), well known oil-water nano-emulsion formulation methods are not amenable to the crosslinked hydrolytically sensitive nanoparticle/nanogel. In this work, a single-phase reaction-precipitation method was developed to formulate quercetin conjugated PβAE nanogels (QNG) via reaction of acrylated quercetin (4 –5 acrylate groups) with a secondary diamine under dilute conditions using acetonitrile as the reaction medium, resulting in a self-stabilized suspension. The proposed approach permits the post synthesis modification of the spherical nanogels with a PEGylated coating, enhancing their aqueous stability and stealth characteristics. Nanogel size was controlled by varying feed reactant concentrations, achieving drug loadings of 25–38 wt%. Uniform release of quercetin over 45–48 hours was observed upon PβAE ester hydrolysis under physiological conditions with its retained antioxidant activity over the extended times.

Graphical abstract

[#]corresponding author dziubla@engr.uky.edu, Tel: +1 859 257 4063, Fax: +1 859 323 1929.

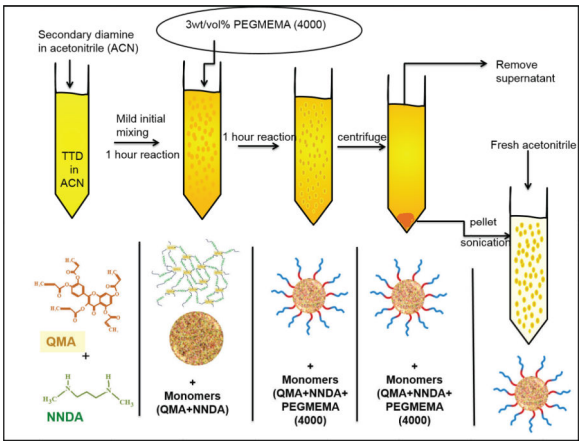

Keywords

Oxidative stress; antioxidants; nanogels; poly (β-amino esters); endothelial cells; quercetin

1. Introduction

Oxidative stress is a pathophysiological condition, where endogenous antioxidants are unable to counteract the production of oxidants, leading to cellular dysfunction. This overproduction of the reactive oxygen and nitrogen species (ROS/RNS) (e.g., hydroxyl radicals, singlet oxygen, hydrogen peroxide, peroxyl radicals) can be caused by both endogenous sources and exogenous sources. Examples of endogenous routes include ROS generating enzymes such as nitric oxide synthase, xanthine oxidase, amplified mitochondrial metabolism especially in aging cells resulting in mitochondrial dysfunction, damaged membrane and hence leakage of ROS into intracellular environment [1–4]. Some of the exogenous sources include exposure to ozone, UV, Y-irradiation, air pollutants penetrating through skin or via inhalation, intake of various drugs, xenobiotic and many more [4–9]. At a systemic level, oxidative stress has been shown to play a role in the development and acceleration of many diseases, including diabetes, cardiovascular diseases, Alzheimer's and Parkinson's disease, acute renal failure, acute lung injury, radiation injury, etc. [10, 11].

Rationally, one would expect that the supplementation of dietary antioxidants would be sufficient to reduce excess ROS into non-reactive stable molecules, resolving the oxidative stress and thereby treating many diseases. In fact, this beneficial property of antioxidants, including polyphenol flavonoids, has been successfully demonstrated *in vitro* multiple times[12, 13]. But despite these *in vitro* demonstrations, nearly all clinical trials with antioxidants have failed to demonstrate substantial benefit [14, 15]. As a result of these outcomes, it has been inferred that a major limitation of dietary antioxidants was their inability to impact the oxidative stress levels in the patients. Given the highly unstable nature of these antioxidants, their typically poor aqueous solubility and lack of natural accumulation in tissues of interest, it is unsurprising that these molecules were unable to perform their intended function. For instance, quercetin has been shown *in vitro* and *in vivo* studies to possess anti-inflammatory [16], anti-hypertensive [17], antiallergic [18] properties

and an ability to control metabolic syndrome [19]. Yet, it has not been used therapeutically for pharmaceutical applications due to its low bioavailability, which is likely due to its poor aqueous solubility, structural instability and extensive first pass metabolism [20, 21]. It has been reported that the oral bioavailability of quercetin is 17% in rats and merely 1% in humans [21, 22]. Moreover, upon intravenous injection, a 100 mg of dose resulted in a 12 μM plasma concentration after 5 minutes and 1 μM after 3 hours, demonstrating the relatively short half-life of the compound [23].

In order to overcome this difficulty of low systemic bioavailability, one potential solution is to deliver quercetin through encapsulation into nanoparticles, which can be administered via a number of routes (e.g., *i.v.*, *s.c*, inhalation, etc.) with an objective of extended drug release and control the rate of first pass metabolism [24]. Several studies have demonstrated the ability to encapsulate quercetin into nanoparticles composed of poly (lactic acid) (PLA), poly (lactic-co-glycolic acid) PLGA, and solid lipid nanoparticles (SLN). These approaches, while potentially useful, possessed significant burst release and low overall drug loading, ranging from only 0.05 to 2 wt% of the total particle weight [25, 26]. Incorporating antioxidants into the backbone of a polymer system could be an alternative towards the effective antioxidant delivery as demonstrated on enzymatically biodegradable poly(trolox) nanoparticle system to deliver trolox, a water soluble analog of vitamin E [27].

Building upon this prior work, it may be possible to overcome drug stability, solubility and drug release limitations by conjugating the drug into the backbone of a hydrolytically biodegradable polymer, such as poly(β-amino esters) (PBAEs), to form pro-drug nanoparticles/nanogels [28, 29]. We have shown previously that antioxidants like curcumin and quercetin can be loaded into crosslinked PBAEs and subsequently released in their original structure upon hydrolysis [30]. But due to the fast reaction kinetics and degradation properties of PβAE, the bulk crosslinking approach is not amendable towards typical nanoparticle synthesis methods (e.g., o/w emulsion polymerization), which use water as a dispersing media. To overcome this problem, we have synthesized quercetin conjugated PBAE gel nanoparticles/nanogels using a single phase reaction-precipitation method in an organic solvent under dilute conditions giving a stable suspension of uniformly sized particles. Covalently reacting available amine groups with poly(ethylene glycol) monomethacrylate resulted in a coating that minimizes post purification instability, expects to reduce the rate of first pass metabolism and serves as an alternative to conventional surfactant based stabilization of nanoparticles. Uniform degradation of these nanogels over 48 hours successfully demonstrated release of active quercetin with negligible burst release. Particle sizes were easy to control with resulting quercetin loading capacities of 25–38 wt%, which possessed biocompatibility equivalent to pure quercetin and were able to suppress cellular oxidative stress over 48 hours.

2. Materials and methods

2.1 Reagents

Quercetin was purchased from Cayman Chemicals, Michigan, USA. Acryloyl chloride, potassium carbonate, N, N’-dimethyl 1–3-propanediamine, polyethylene glycol methyl ether methacrylate (Mn=4000) (PEGMEMA4000), potassium persulfate, 2, 2’-azino-bis (3-

ethylbenzothiazoline-6-sulphonic acid), hydrogen peroxide were purchased from Sigma Aldrich. IgG antibody was purchased from Jackson Immuno Research Laboratory Inc. For cell culture studies, EBM basal medium (phenol red free), EGM-2 growth factors, and Human Umbilical Vein Endothelial Cells were purchased from Lonza. Calcein-AM red-orange and 2', 7 dichloro-dihydrofluorescein diacetate (H_2DCFDA) were purchased from Life Technologies. Iodogen® iodination reagent (1, 3, 4, 6-tetrachloro-3α-6α-diphenylglycouril) was bought from Thermo Scientific, Rockford, IL.

2.2 Quercetin functionalization to quercetin multiacrylate (QMA) monomer

Quercetin multiacrylate (4–5 acrylate groups per molecule) (QMA) was prepared in accordance with the protocol described by Wattamwar et. al. [31] with slight change of using potassium carbonates as the acid capturing agent instead of triethylamine. Briefly, reaction between quercetin (20gms in 200ml of THF) and acryloyl chloride was carried out in anhydrous THF. Potassium carbonate was added to the reaction system to capture the hydrogen chloride forming its salt as the reaction byproduct. System was purged with nitrogen for 30 minutes initially and then was further allowed to react overnight at room temperature to functionalize quercetin phenolic groups into acrylate. Acryloyl chloride and potassium carbonate, both were added in the molar ratio of 1:1.2 with respect to the phenolic groups present in quercetin. Quercetin has four phenolic groups, which can be actively functionalized. Therefore, for every mole of quercetin, five moles of acryloyl chloride and potassium carbonate were added to the reaction medium. Acrylated quercetin solubilizes in THF as the reaction proceeds. After the reaction, solubilized product was first filtered out to remove the salts. Subsequently, dissolved product was vacuum dried to remove all the THF and was re-dissolved in DCM in order to carry out aqueous-organic solvent extraction process to remove any unreacted acryloyl chloride/acrylic acid and quercetin. A basic solution of 0.1 M potassium carbonate in DI water was used as the extraction medium for acrylic acid and quercetin both. After extraction, magnesium sulfate was added to the product solubilized in DCM to remove any remains of water. Finally the pure QMA was obtained as a dry product after evaporation of DCM overnight. Characterization of the functionalized quercetin was completed using ^{1}H-NMR and mass spectroscopy to identify the number of acrylate groups per molecule of quercetin (Figure 2 and 3 and Table 1 in supplement information).

2.3 Quercetin PBAE nanogel (QNG) synthesis

Quercetin PBAE nanogels were prepared using a single-pot dilute synthesis approach. QMA was dissolved in anhydrous acetonitrile to specified concentrations of 0.75, 1.25, 2.5, 5 and 10 mg/ml. A stock solution of N, N'dimethyl-1–3 propane diamine (NNDA, a secondary diamine) (100 mg/ml) was prepared in acetonitrile. Calculated volume of NNDA stock: 3.67, 6.12, 12.25, 24.5, and 49 μl was added to the reaction solutions with QMA concentrations: 0.75, 1.25, 2.5, 5 and 10 mg/ml respectively to achieve the required reaction concentration, maintaining stoichiometric ratio of acrylate to reactive amine at 1:1.1. QMA-NNDA reaction in these diluted conditions resulted in precipitation into nanogel form. These quercetin-PBAE nanogels will be further referred as QNG (0.75), QNG (1.25), QNG (2.5), QNG (5), and QNG (10) for different systems with feed QMA concentrations of 0.75, 1.25, 2.5, 5 and 10 mg/ml respectively. Reaction time of the nanogel synthesis was determined by

analyzing the reaction supernatant at different time point to observe the decrease in QMA absorbance peak. After 45 minutes of reaction, peak intensity does not change. Therefore, the reaction was carried out for one hour, resulting in precipitated nanogels. Hydrodynamic radius of the synthesized nanogels in acetonitrile was determined using dynamic light scattering (DLS) (Malvern Zetasizer (ZS 90)). Appropriate dilution using fresh acetonitrile were used in order to get the count rate between 200 to 300 cps. Hydrodynamic diameter was reported as z-average. All the parameters were set for acetonitrile medium at 25 °C.

After the completion of the reaction, 63 μl (32 mg) of a concentrated solution (500 mg/ml) of polyethylene glycol methyl ether methacrylate 4000 (PEGMEMA4000) in acetonitrile was added to 1 ml of the nanogel suspension along with gentle mixing for few seconds to get 3% wt/vol PEGMEMA4000 in suspension. This system was allowed to react for one hour, followed by centrifugation at 6700 rpm for 10 minutes. The pellets were re-suspended in a fresh acetonitrile by sonication for 3–5 minutes. Particles were then centrifuged and nanogels pellets were freeze-dried and stored at −80°C for further analysis.

Nanogels were also synthesized at variable acrylate to reactive hydrogen amine stoichiometric ratios ranging from 0 to 10, in order to study the effect of reactant molar ratio. For this system, QMA feed concentration was kept constant at 2.5mg/ml and amine content was varied. Nanogel suspension obtained from each ratio was diluted with DMSO, in order to dissolve any precipitated quercetin due to excess amine. Size of the nanogels in suspension was measured using DLS after adjusting the instrument parameters according to the suspension medium.

2.4 Size and yield of nanogel synthesis reaction

In order to determine reaction yield, the concentration of unreacted QMA in supernatant obtained after first centrifugation was measured, via UV-VIS spectroscopy. The sample was prepared by diluting 100 μl of supernatant with 1 ml of acetonitrile. The absorbance of diluted solution was measured at 350nm using UV-VIS spectrophotometer (Varian Cary 50 Bio UV-Vis spectrophotometer). The amount of unreacted QMA was calculated using a calibration of pure QMA dissolved in acetonitrile and percent QMA reacted or yield was back calculated subsequently. Size of the nanogels was measured using DLS at different stages of synthesis.

2.5 SEM imaging

In order to determine particle morphology, scanning electron microscopy was performed on the synthesized nanogels. 50 μL of PEG coated nanogel suspension in acetonitrile (synthesized using 2.5mg/ml feed QMA concentration) was diluted to 1 ml with acetonitrile and pulse sonicated 8– 10 times in 2–3 second pulses at 2–6 watts. A drop of the solution was dried on gold plated surface overnight in the bio-hood and covered with Kim wipes as an added precaution to prevent dust settling. Next day the dried sample on a gold surface was sputter coated with gold-palladium alloy and images were taken at various magnifications using S-4300 Hitachi Scanning Electron Microscope.

2.6 Analysis of enhanced stability of nanogels after the reaction with PEGMEMA4000

To determine the impact of PEGMEMA4000 treatment on nanogels stability, particle size was analyzed at two stages, first before the PEGMEMA4000 reaction and second after the PEGMEMA4000 reaction. To prepare the samples, 50 μL of nanogel suspension was added to 1 ml of PBS (pH=7.4) to form a suspension. Size measurement of the suspended nanogels in PBS was carried out using DLS without any further agitation at an interval of 10 minutes for a total time of 50 minutes and recorded to analyze the effect of PEGylation. The size measurement was done for nanogels obtained at both the stages described above. Nanogels were also treated with only polyethylene glycol) methyl ether Mn=5000 (PEGME5000) for 1 hour and analyzed for the size afterwards.

2.7 PEG content analysis after nanogel formulation

Analysis of PEG content in nanogels was performed using the barium-iodide assay [29]. To carry out the assay, two solutions were prepared. A) 60 mg/ml barium chloride in 1.2 N HCl (HCl stock diluted in DI water), B) potassium iodide and iodine in DI water with final concentration of 20 and 12.5 mg/ml respectively. Separately, 1 mg of nanogels was rapidly hydrolyzed in 500 μL of 5 N NaOH for 4 hours at 80o°C. Hydrolyzed nanogels were neutralized by addition of 500 μL of 5 N HCL. PEGMEMA4000 dissolved in DI water was used for standard calibration within the range of 0–10μg per well in a 96 well plate. 20 μL of the hydrolyzed nanogel solution was added to the wells. Sample and the calibration volumes were diluted to 170 μL with DI water. 40 μL of solution A was then added to each well followed by mixing. 40 μL of solution B after doing 1/5th dilution was added subsequently to all the wells and mixed. The reaction was allowed to develop for 10 minutes after which absorbance was recorded at 550 nm using Varian Cary 50 Bio UV-Vis spectrophotometer. Calibration curve of PEG (5000 MW) was used as a calibration standard.

2.8 Antibody Binding studies of Q-PBAE nanogels using IgG using radiolabeling

^{125}I-IgG stock preparation—IgG was radiolabeled with ^{125}I to serve as a tracer to protein bound to the nanogels. Briefly, 200μL of 2mg/ml Iodogen® iodination reagent (1, 3, 4, 6-tetrachloro-3α-6a–diphenylglycouril) in chloroform was dried in a glass tube using dry nitrogen gas to form a thin layer on the glass wall. 100μL of 1mg/ml Mouse IgG was added to iodogen coated tube and radioactive iodine (Na^{125}I) was added and incubated for 5 minutes. Free iodide was removed from the protein using a Thermo Scientific protein desalting spin column according to manufacturing instructions. Any free iodine remaining in the spun down solution was determined using trichloroacetic acid (TCA) precipitation. Gamma counts of both the precipitate and supernatant were analyzed using Perkin Elmer 2470 automatic gamma counter. Amount of free iodine in hot IgG was found to be 5.6%.

IgG binding to quercetin nanogels—Three different formulations of QNG were used: QNG (0.75), QNG (1.25), and QNG (2.5). IgG having 2 wt% *^{125}I-IgG* was added to the nanogels (with and without PEG coating) suspended in PBS. Final concentrations of IgG and nanogels in the buffer were maintained at 1.17 and 0.4 mg/ml respectively. After 3 hours of incubation, the suspension was then centrifuged at 6700g for 20 minutes to collect

the pellet at the bottom and supernatant from the top. Both pellet and the supernatants of all the nanogel formulation were analyzed using gamma counter.

2.9 Quercetin release profile of Q-PBAE nanogels in PBS

QNGs were suspended in PBS buffer (pH=7.4) using probe sonication to a concentration of 1mg/ml. As quercetin has very limited aqueous solubility, degradation buffer was prepared using 2 vol% DMSO in order to solubilize any released quercetin during hydrolytic degradation. This suspension was incubated at 37°C in a shaker bath at 70 RPM. Every 2 hours, nanogel suspensions were centrifuged at 6700 RCF for 10 minutes and the supernatant was collected and stored at −20°C for further analysis. The centrifuged pellet was re-suspended in fresh buffer to continue degradation. Supernatant's absorbance was measured at 370nm using Varian Cary 50 Bio UV-Vis spectrophotometer to determine the amount of quercetin released. Degradation was carried out for 50 hours and quercetin concentration in supernatants were analyzed after each collection.

2.10 *In vitro* antioxidant activity capacity of the degradation products of nanogels

Antioxidant activity of released quercetin and degradation products was evaluated using the Trolox Equivalent Antioxidant Capacity (TEAC) assay, which is based on scavenging of 2, 2'-azinobis-(3- ethylbenzothiazoline-6-sulfonate) radical anions (ABTS-). Briefly, 7mM ABTS radical cation stock solution was prepared by mixing 1 ml of 8 mg/ml of ABTS solution with 1 ml of 1.32 mg/ml of potassium persulfate solution, both prepared in DI water. This solution was allowed to react overnight to form ABTS radical cation stock solution. After 24 hours, ABTS radical cation working solution was prepared by diluting the stock solution in PBS to an absorbance of 0.4 at 734 nm. For calibration purpose, standard solution of trolox of known concentrations (0 to 0.27 mM) in PBS were prepared and used for the assay. To carry out the TEAC assay, 10 μL of test sample (degradation supernatants/ trolox standards) was added in a 96-well plate. Subsequently, 200 μL of the ABTS radical cation working solution was added to all the wells. After 5 minutes absorbance of all the samples was measured at 734 nm. Trolox standard curve with respect to the obtained absorbance was prepared and equivalent trolox concentration in the samples was calculated using trolox calibration curve. The equivalent quercetin concentrations were calculated by obtaining TEAC value of pure quercetin using the same assay.

2.11 Cell toxicity study of quercetin nanogels on Human Umbilical Vein Endothelial Cells (HUVECs)

HUVECs were cultured in EBM basal medium (phenol red free) with EBM-2 growth factors to an 80% confluence in 48-well plate overnight. A range of concentrations (from 1 to 70 μg/ml of equivalent quercetin content) of nanogels in media were prepared and added to the well plate (n=4). After 24 hours, treated and non-treated control cells were washed with fresh media followed by incubation in 1mM Calcein AM red-orange live cell tracer. After 1 hour, cells were washed again with fresh media once, followed by addition of fresh media. Fluorescence was recorded at excitation/emission of 540/590 nm using BioTek Synergy Mx, Gen5 2.0, Winooski, VT to analyze the cell viability.

2.12 Cellular oxidative stress suppression

HUVECs were cultured in 48 well plate in EBM basal medium with EBM-2 growth factors. In order to determine the ability of Q-PBAE nanogels to block oxidative stress injury, HUVECs exposed to hydrogen peroxide (0.5mM) were treated with free quercetin and nanogels (QNG (1.25)) with equivalent quercetin concentrations of 5 and 10μg/ml. DCF-DA to a final concentration of 10 μM was added at the time of treatment and DCF fluorescence was used as a measure of oxidative stress levels in the cells. Three similar 48 well plates prepared. DCF fluorescence at 490/525 nm and cell viability was measured at 24 and 48 hours using BioTek Synergy Mx, Gen5 2.0, Winooski, VT.

3. Results

3.1 Hydrodynamic radius and yield of reaction of Q-PBAE nanogels

The hydrodynamic diameter of the nanogels was determined using DLS before and after PEGylation. The extent of reaction was evaluated by UV-Vis spectrophotometer. As the concentration of reactants increased, nanogels size increased from about 250±6 to 600±21 nm, and reaction yields increased from 81±2.6 % to 92±0.54 % (Figure 1). A slight increase in nanogel diameter (approximately 50 nm) was observed after the reaction with 3wt/vol% of PEGMEMA4000. This increase can likely be attributed to the attachment of PEG chains at the surface of nanogels as shown in schematic (Schematic 1).

3.2 Analysis of shape and size of nanogels

Nanogels prepared using 2.5 mg/ml feed QMA concentration were imaged in SEM to examine shape and size. Nanogels with diameter ranging from 100–250 nm with an average of 197±57 nm as analyzed using Image J software were observed (Figure 3a, b). The nanogels' spherical morphology was confirmed by imaging at an angled view at 38° (Figure 3, c and d). There was an observed phenomenon of fusion at the nanogel surface as they are soft polymeric particles, which might be undergoing interfacial attraction forces during solvent evaporation on the gold substrate.

3.3 Effect acrylate to amine ratio on nanogels size (stoichiometric feed ratio)

Different acrylate to amine ratios were investigated to study the effect of stoichiometric ratios on nanogel diameter and reaction yield. Because of the possibility that higher amount of amine can result in hydrolysis of QMA and precipitation of quercetin, 200μL of DMSO was added to each 1 ml suspension of nanogels to dissolve any precipitated quercetin but not crosslinked nanogels. It was observed (as shown in figure 4), the highest hydrodynamic diameter (311 nm) as well as yield of the reaction (89%) was obtained with acrylate to reactive amine hydrogen ratio of 1:1.1 while higher or lower ratio resulted in smaller sizes with either incomplete reaction of QMA or precipitation of nascent quercetin. For all further studies, QNGs were synthesized with feed ratio of 1:1.1, which results in slightly excess of amine, which permits conjugation of the PEGMEMA4000 system

3.4 Analysis of enhanced stability of nanogels after the reaction with PEGMEMA4000

PEGylation of nanogels with PEGMEMA4000 resulted in the physical stability of nanogel suspension in aqueous media (PBS. pH=7.4). As shown in figure 5, PEGMEMA4000 treated retained their size from 373±5.8 at t=0 to 364±68 after 50 minutes of suspension. This could be due to the stearic hindrance of the PEG groups that leads to the formation of stable suspensions in contrast to non-PEGylated nanogels that aggregated with time in PBS giving size of over 1 micron within 20 minutes. Incubation of nanogels with PEGME5000 did not result in their stability in PBS either but in aggregation of nanogels over time with observed diameter of 2.5 μM within 50 minutes of suspension, confirming that the stability of nanogels after PEGylation is due to the covalent bonding of PEG to its surface due to the reaction of mono acrylate from PEG with unreacted terminal amine hydrogen of the nanogels.

3.5 Nanogel PEGylation and protein binding

PEG content in the nanogels has been represented as PEG weight percent in the total nanogel mass shown in figure 6. It was observed that nanogels synthesized from lower QMA feed concentrations of 0.75 and 1.25 mg/ml had 40.7 and 30.4 wt% PEG respectively, while the higher concentration systems, 2.5, 5, and 10 mg/ml, had lower PEG content at 7.6, 1.23 and 3.1 wt% respectively and influence of this variable PEG content was seen in the IgG binding capacity as discussed below.

While nanogels with non-PEG coated system showed high IgG binding, 59.8±1.6, 73.84±2.1 and 71.25±1.2 % surface covered for QNG (0.75), QNG (1.25) and QNG (2.5), respectively. PEG coated nanogels with same formulations showed a substantial decrease in IgG binding, 18.4±4.8, 37.3±7.4 and 50.6±5.4 % surface coverage for QNG (0.75), QNG (1.25) and QNG (2.5), respectively (Figure 7, bar chart). Additionally, as the PEG weight percent decreased, the percent IgG bound increased, indicating the presence of a PEG coating of the nanogels (Figure 7, line graph).

3.6 Quercetin release profile and antioxidant activity

Figure 8a,b shows the released products and degradation profile of the nanogels in PBS at 37°C. Supernatants containing the degradation products were analyzed using UV-Vis spectroscopy. Quercetin release was linear for the first 36 hours, followed by a plateauing profile, with approximately 95% total release in 35–40 hours. These nanogels had minimal burst release, of 11.93±1.5, 4.43±0.4, 6.8±0.27, 9.3±1.6, 9.9±0.97 % for QNG (10), QNG (5), QNG (2.5), QNG (1.25) and QNG (0.75), respectively. This low level is likely due to unconjugated quercetin in the gel matrix. Taking into account the first 60% of the total release, profiles were fit to the Korsmeyer-Peppas model ($M_t/M_{inf} = Kt^n$) for the *in* vitro release model fit [32, 33]. To identify between the diffusion, anomalous and erosion controlled release regimes, exponent ‘n’ values were identified. For a spherical system, n=0.43 implies pure diffusion, n=0.85 suggests erosion and 0.43<n<0.85 implies anomalous transport or a combination of diffusion and erosion. With the ‘n’ values of 0.55, 0.85, 0.69, 0.58 and0.58 for QNG (10), QNG (5), QNG (2.5), QNG (1.25) and QNG (0.75) respectively, indicates the anomalous diffusion release mechanism of nanogel degradation according to the model defined. R^2 values were within the range of 0.97–0.99. Since similar

release profiles were seen for all formulations irrespective of the different nanogels formulations, which gave varied nanogel diameter and given the swellable nature of PβAE polymer, bulk erosion phenomena is likely to happen via hydrolysis instead of surface erosion for these systems. Figure 8(a) represents the HPLC chromatograms of quercetin, quercetin multiacrylate and degradation products of Q-PβAE bulk gel system and nanogel systems. HPLC Analysis of degradation products of Q-PβAE bulk gels (#3) in the, (figure 8(a)) identified release of both quercetin and the monoacrylate form. However, degradation products of the synthesized Q-PβAE nanogels (#4)) resulted in the release of pure quercetin, with no detectable trace of mono or higher acrylate products, confirming the retrieval of original drug. Meanwhile, TEAC studies of the degraded product indicated that the released compounds possessed antioxidant activity against free radicals for 36–40 hours (Figure 8 (c)) and possessed a similar release profile as obtained from degradation product UV Vis analysis. Equivalent active quercetin was also calculated for each time point taking 4.2 as the TEAC value of quercetin. It was observed that equivalent active quercetin either complied with the released quercetin or higher than that implying no loss of quercetin activity while degradation and release. Higher values of equivalent active quercetin is likely from oligomers released during hydrolysis and degradation products of quercetin, which also have some inherent antioxidant activity. Taken together, quercetin was successfully kept intact within the polymer matrix for an extended period of time without loss of activity. This result is in contrast to the usual behavior of quercetin, where structural stability and antioxidant activity is lost within 2 hours of incubation in aqueous media.

3.7 Nanogels with Human Umbilical Vein Endothelial Cell (HUVECs) line

3.7.1 Dose dependent cell toxicity—Potential cytotoxicity of quercetin-based nanogels in biological environment was analyzed by exposing HUVEC monolayers to quercetin nanogels. The cells were exposed to equivalent quercetin concentrations ranging from 1 to 70 μg/ml of nanogels for 24 hours (and 48 hours - see supplement) followed by treatment with Calcein AM red-orange (fluorescent cell tracer), as a measure of cell viability. Calcein AM red-orange was used as it does not interfere with the fluorescence of quercetin itself. As shown in figure 9, cell viability starts to decrease to about 50% at 70 μg/ml of equivalent quercetin concentrations. All nanogel formulations showed similar viability trends when compared within themselves as well as when compared with pure quercetin for both 24 and 48 hours exposure times. This was confirmed after conducting two-way ANOVA test considering nanogel composition and treatment concentrations as two groups. The two-factor analysis of variance showed no significant effect of composition towards cell viability but dose dependent cytotoxic effect was statistically different after 24-hour and 48-hour treatment. This demonstrates that presence of PβAE nanogels or its degradation products apart from quercetin did not contributes to cell cytotoxicity.

3.7.2 Effect of nanogels on H_2O_2 treated HUVECs for 24 hours—HUVECs at 80% confluence were treated with two different concentrations of QNG-1.25 (5 and 10 μg/ml equivalent quercetin concentration) and 0.5 mM H_2O_2 as an inducer of cellular injury and oxidative stress . 10 μM DCFDA was added to each well. Cell viability and DCF fluorescence were measured at 24 and 48 hour and compared with the no particle treatment and no H_2O_2 controls. Cell viability was maintained on a concentration basis for only

quercetin/QNG treatment after 48 hours. A slight increase in viabilities was seen after 48 hours with the antioxidant treatments (Figure 10(a) and 10 (b)). When looking at DCF fluorescence for the same treatment system, antioxidant treatment suppressed the background oxidative stress to a significant level at both 24 and 48 hours when compared with no treatment controls (Figure 11 (a)). External oxidative stress induced using H_2O_2, as shown in figure 11 (b), resulted in cell viability dropping to 10% after 24-hour exposure 20% after 48 hour exposure. . H_2O_2 exposed groups treated with free quercetin or QNG showed different responses after 24 and 48 hour exposure. For 24 -hour, all the treatments with either free quercetin or QNGs, showed same protection from H_2O_2 with cell a viability of approximately 50%. With 48-hour exposure study, though we saw equivalent protection from both free quercetin and QNG with 5 μg/ml, QNGs at 10 μg/ml showed improved performance than just quercetin despite of having same inherent toxicity at that concentration. Suppression of DCF fluorescence at both 24 and 48 hours for 10 μg/ml QNG system was superior to pure quercetin.

4. Discussion

Numerous trials have been conducted over the years evaluating the continuous administration of antioxidants and their effect on chronic diseases like atherosclerosis or diabetes. Yet, results have been inconclusive and debatable towards their beneficial effects [34]. However, as the use of antioxidants in sub-acute inflammatory diseases (e.g., n-aceytl cysteine in acetaminophen toxicity) have shown clinical acceptance, there must be something more to this observed discrepancy [35]. One explanation for the better *in vivo* performance of n-acetyl cysteine in this setting is the improved natural accumulation in the intended site of action (e.g., the liver) and more favorable circulation times over that of other antioxidants, which has a half-life of 6 hours compared to minutes for many polyphenolic antioxidants [36, 37]. However the use of N-acetyl cysteine is also complicated with side effects common of sulfur containing compounds, including nausea, vomiting and risk factors of asthma, drug allergy etc. [38]. As such, it may be possible to rescue small antioxidant therapy for short-term oxidative stress disorders through changing their inherent pharmacokinetics.

The objective of this work was to design a biocompatible polymeric nanocarrier capable of systemically delivering highly active though labile antioxidant, quercetin, over an extended period of time to fight acute oxidative stress conditions. We have incorporated PβAE gel synthesis chemistry in making quercetin conjugated PβAEs nanogels. Our lab group and other researchers have previously reported successful synthesis of PβAE bulk hydrogels using different co-monomers including polyphenolic antioxidants along with PEGDA and DEGDA [31, 39, 40]. By taking advantage of polyphenolic structure, quercetin can be acrylated, which when reacted with an amine can form crosslinked gel via Michael addition mechanism. However, due to rapid kinetics and multifunctional nature of the monomer, translation from bulk gel to nanogel is a technically challenging hurdle. Owing to the hydrolytically degradable property of PβAEs, standard two-phase (oil-water or oil-oil) emulsion techniques are not feasible. However, by formulating quercetin-PβAE nanogels (QNG) via single-phase reaction-precipitation method in acetonitrile under dilute conditions, resulted in nanogel suspension as reaction proceeded to completion, spherical nature of

which was confirmed by SEM imaging (Fig 3). The presence of excess available terminal amines permitted the covalent linkage of PEG monoacrylate grafts to the nanogel resulting in more stable coating when compared with conventional surfactant or any other lipophilic molecule stabilization methods. As PEG grafts are able to stearically stabilize nanoparticles, PEGylation of the nanogels enhanced their post-purification stability and improved their stealth characteristics. The single-phase reaction systems/ one-pot synthesis simplified the synthesis process, eliminating the requirement of any stabilizer and its excess removal during purification. A very simple purification step of centrifugation was used, after which nanogels restored their original size without any aggregation (Schematic 1, figure 2). PEGylation improved the stability in organic aqueous solutions. This is in contrast to QNGs incubated with PEGME5000 (MW in the range similar to PEGMEMA4000). The lack of the acrylate group prevented covalent addition to the particles and was therefore unable to prevent particle aggregation (Fig 6). This confirms the presence of covalent linkage between PEG acrylate group and NNDA unreacted terminal hydrogen amines, which eventually results in QNG physical stability.

Precise control of nanogel size was made possible by varying the feed reactant concentration while keeping the stoichiometric ratio constant, with increasing concentration increasing particle size (Fig2). Interestingly, as the ratio of acrylate to amine decreased, the excess amine catalyzes the hydrolysis of the acrylate groups. To minimize the occurrence, the stoichiometric ratio of acrylate to reactive hydrogen amine was limited to 1:1.1 which still offered maximum reaction yield, diameter and provides the opportunity to covalently bind PEGMEMA4000 to terminal amines (Fig 4). It was observed that after using same concentration of PEGMEMA4000 for all formulations, the smaller nanogels had higher amount of PEG attached (30–40% wt/wt) while the larger diameter nanogels had PEGylation of only 3–5 wt% (Fig 5). This could be due to the presence of more amine reactive sites on smaller particles due to overall higher surface area for the same quantity. The PEG presence was further substantiated by performing a radiolabeled-IgG binding studies where reduced amount of IgG binding was observed for PEGylated nanogels as opposed to non-PEGylated nanogels (Fig 7). Also as wt% of PEG decreased with different nanogel formulations, percent IgG bound increased clearly implying that presence of PEG was altering the anti-body binding effect in a positive fashion.

These hydrophobic polymeric quercetin-PBAE systems are hypothesized to degrade in PBS via hydrolysis of ester bond to release quercetin. This was confirmed by injecting degradation products through HPLC where we saw the most significant elution peak coinciding with pure quercetin peak with no oligomer or other forms of quercetin acrylate present (Fig 8 (a)) confirming the presence of original quercetin molecule in the degradation product. Nanogels showed uniform degradation over 48 hours with about 5–10% of the total quercetin released in first 30 minutes as analyzed by UV-Vis (Fig 8(b)). While the Korsmeyer-Peppas (K-P) release profile model for spherical systems with $0.43<n<0.85$ suggests the contribution of diffusion as well as erosion based degradation, similar release profile of all the formulations (QNG (0.75)-QNG (10)) with variable diameter confirms the bulk erosion instead of surface erosion degradation mechanism, (Fig 8(b)). An important fact to notice in the release profile is that the value of ‘n’ obtained using the K-P model closely correlates with the percent burst release considering it to occur at 1st sampling time

point of 30 minutes. The system with highest burst release of 11.93% (QNG (10)) fits with the ‘n’ value of 0.55 (near diffusion boundary) while QNG (5) with lowest burst release of 4.43% amongst all the systems gives the ‘n’ value of 0.85 (pure erosion mechanism). This trend of higher burst release with lower ‘n’ value clearly implies that the diffusion contribution in the release model is largely coming due to the unconjugated quercetin being diffused through the spherical gel matrix at early time points while the quercetin released due to the ester hydrolysis is derived by erosion based mechanism. Analyzing the antioxidant activity of the released products using TEAC assay confirmed that the products released at 24 hour or 48 hour still possess antioxidant activity and quercetin conjugated to PBAE backbone was structurally intact even after being incubated in aqueous media for several hours (Fig 8(c)). Comparing the equivalent quercetin amount obtained from TEAC assay and actual quercetin release in figure 8(c), it is clear that the nanogel degradation products are showing higher activity than would be estimated through pure quercetin release (Fig 8(d)). One explanation for the persistent excess activity throughout the degradation process could be due to the auto-oxidation or molecular degradation of the released quercetin in aqueous environment resulting in metabolized fragments such as phloroglucinol, protocatechuic acid etc. These small fragmented molecules though not quantifiable at same wavelengths as quercetin have some potential towards free radical scavenging which could be contributing towards ABTS radical consumption in the TEAC assay [41]. Hence, even the fragmented degradation products contributed to the total antioxidant potential of the system over time.

As a pharmaceutically active compound, quercetin like any other therapeutic compound has a window of safety with TC50 value of 0.23 mM or ~ 70 jag/ml (Fig 9(a)). When loaded into a drug carrier system, it is important to investigate the potential toxicity of the carrier system along with the loaded drug. As literature for PβAE systems indicate low relative toxicity *in vitro and in vivo*, it is expected that quercetin PβAE nanogels would have the similar safety window as for pure quercetin with no added effect due to the polymer backbone. This was confirmed with the dose dependent cytotoxicity study of all the QNG systems and when compared with quercetin, QNGs toxicity patterns the cytotoxic profile of quercetin directly confirming once again the viable nature of PβAE nanogel by itself (Fig 9 (a) and (b)). These nanogels were further evaluated for their ability to suppress oxidative stress due to external injury induced using 0.5 mM H_2O_2 exposure. They not only showed ROS scavenging capacity against H_2O_2 induced injury as good as pure quercetin at equivalent quercetin loading of 5 μg/ml, but the treatments done with QNGs having 10 μg/ml of equivalent quercetin loading showed enhanced protection against oxidative stress as compared to nascent quercetin after 48 hours probably due to prolonged supply of active quercetin during nanogel degradation. This was verified by both viability and DCF fluorescence studies showing superior properties of QNGs than pure quercetin even though present in same quantities (Fig 11(b)). Therefore, with the ability to suppress oxidative stress *in vitro*, slow uniform release and longer circulation efficacy, these nanogels can serve as an effective delivery system for therapeutically potential yet fragile antioxidant, quercetin, which shows very low bioavailability *in vivo* otherwise.

5. Conclusions

Nanogels were synthesized using a novel but simple single-phase reaction-precipitation system with control over the size through varying feed reactant concentrations. These nanogels were able to be PEGylated post synthesis through secondary Michael addition reaction with available amines on the nanogel surface, resulting in decreased opsonization. The PBAE chemistry to chemically conjugate quercetin protects quercetin from losing antioxidant activity until the polymer degrades and releases the quercetin. To the best of our knowledge, these nanogel systems when compared with other nanocarriers have the highest reported quercetin drug loading. The uniform, prolonged release of quercetin from QNGs due to hydrolytic cleavage showing equivalent antioxidant activity as pure quercetin potentially shows protection against induced oxidative stress for as long as 48 hours.

Supplementary Material

Refer to Web version on PubMed Central for supplementary material.

Acknowledgements

The project described was supported by a grant from the Office of Naval Research (ONR DEPSCoR) and the National Center for Research Resources and the National Center for Advancing Translational Sciences, National Institutes of Health, through Grant UL1TR000117. The content is solely the responsibility of the authors and does not necessarily represent the official views of the Office of Naval Research or the NIH.

Abbreviations

ABTS	2, 2’-azinobis-(3- ethylbenzothiazoline-6-sulfonate)
DCF-DA	Dichlorofluorocein-diacetate
DEGDA	Diethylene glycol diacrylate
DLS	Dynamic light scattering
DMSO	Dimethyl sulfoxide
EBM	Endothelial basal medium
HCl	Hydrogen chloride
HPLC	High pressure liquid chromatography
HUVEC	Human umbilical vein endothelial cell
IgG	Imunnoglobin G (antibody)
NNDA	N, N’ dimethyl 1, 3-propane diamine
PBAE	Poly (β-amino esters)
PBS	Phosphate buffer saline
PEG	Poly ethylene glycol
PEGDA	Polyethylene glycol diacrylate

PEGME5000	Poly ethylene glycol methylether, Mn~5000
PEGMEMA4000	Poly ethylene glycol methylether methacrylate, Mn~4000
PLA	Poly (lactic acid)
PLGA	Poly (lactic-co-glycolic acid)
QMA	Quercetin multiacrylate
QNG (x)	Quercetin conjugated PBAE nanogels (feed QMA concentration)
RNS	Reactive nitrogen species
ROS	Reactive oxygen species
SLN	Solid lipid nanoparticles
TCA	Trichloroacetic acid
TEAC	Trolox equivalent antioxidant capacity
THF	Tetrahydrofuran
TNF-α	Tumor necrosis factor-α

References

1. Shigenaga TMH MK, Ames BN. Oxidative damage and mitochondrial decay in aging. Proceedings of the National Academy of Sciences of the United States of America. 1994; 91:10771–10778. [PubMed: 7971961]
2. Richter C, Gogvadze V, Laffranchi R, Schlapbach R, Schweizer M, Suter M, et al. Oxidants in mitochondria: from physiology to diseases. Biochim Biophys Acta. 1995; 1271:67–74. [PubMed: 7599228]
3. Canas PE. The role of xanthine oxidase and the effects of antioxidants in ischemia reperfusion cell injury. Acta physiologica, pharmacologica ettherapeutica latinoamericana : organo de la Asociacion Latinoamericana de Ciencias Fisiologicas y [de] la Asociacion Latinoamericana de Farmacologia. 1999; 49:13–20.
4. Kohen R, Nyska A. Invited Review: Oxidation of Biological Systems: Oxidative Stress Phenomena, Antioxidants, Redox Reactions, and Methods for Their Quantification. Toxicologic Pathology. 2002; 30:620–650. [PubMed: 12512863]
5. Jacobs H, Moalin M, van Gisbergen MW, Bast A, van der Vijgh WJ, Haenen GR. An essential difference in the reactivity of the glutathione adducts of the structurally closely related flavonoids monoHER and quercetin. Free radical biology & medicine. 2011; 51:2118–2123. [PubMed: 21982895]
6. Bhalla DK. Ozone-induced lung inflammation and mucosal barrier disruption: toxicology, mechanisms, and implications. Journal of toxicology and environmental health Part B, Critical reviews. 1999; 2:31–86.
7. Pentland AP. Active oxygen mechanisms of UV inflammation. Advances in experimental medicine and biology. 1994; 366:87–97. [PubMed: 7771293]
8. Koren HS. Associations between criteria air pollutants and asthma. Environmental Health Perspective. 1995; 103:235–242.
9. Naito Y, Yoshikawa T, Yoshida N, Kondo M. Role of oxygen radical and lipid peroxidation in indomethacin-induced gastric mucosal injury. Digestive diseases and sciences. 1998; 43:30s–34s. [PubMed: 9753223]
10. Poulsen HE. Oxidative DNA modifications. Experimental and toxicologic pathology : official journal of the Gesellschaft furToxikologische Pathologie. 2005; 57(Suppl 1):161–169.

11. Ghibu S, Delemasure S, Richard C, Guilland JC, Martin L, Gambert S, et al. General oxidative stress during doxorubicin-induced cardiotoxicity in rats: absence of cardioprotection and low antioxidant efficiency of alpha-lipoic acid. Biochimie. 2012; 94:932–939. [PubMed: 21396425]
12. Magalhaes LM, Segundo MA, Reis S, Lima JLFC. Methodological aspects about in vitro evaluation of antioxidant properties. Analytica Chimica Acta. 2008; 613:1–19. [PubMed: 18374697]
13. Huang D, Ou B. Prior RL The Chemistry behind Antioxidant Capacity Assays. Journal of Agricultural and Food Chemistry. 2005; 53:1841–1856. [PubMed: 15769103]
14. Halliwell B. The antioxidant paradox: less paradoxical now? British Journal of Clinical Pharmacology. 2013; 75:637–644. [PubMed: 22420826]
15. Rigg JL, Elovic EP, Greenwald BD. A review of the effectiveness of antioxidant therapy to reduce neuronal damage in acute traumatic brain injury. The Journal of head trauma rehabilitation. 2005; 20:389–391. [PubMed: 16030445]
16. Perez-Vizcaino F, Duarte J, Jimenez R, Santos-Buelga C, Osuna A. Antihypertensive effects of the flavonoid quercetin. Pharmacol Rep. 2009; 61:67–75. [PubMed: 19307694]
17. Galisteo M, Garcia-Saura MF, Jimenez R, Villar IC, Zarzuelo A, Vargas F, et al. Effects of chronic quercetin treatment on antioxidant defence system and oxidative status of deoxycorticosterone acetate-salt-hypertensive rats. Molecular and cellular biochemistry. 2004; 259:91–99. [PubMed: 15124912]
18. Bucki R, Pastore JJ, Giraud F, Sulpice JC, Janmey PA. Flavonoid inhibition of platelet procoagulant activity and phosphoinositide synthesis. Journal of thrombosis and haemostasis : JTH. 2003; 1:1820–1828. [PubMed: 12911599]
19. Lee ES, Lee HE, Shin JY, Yoon S, Moon JO. The flavonoid quercetin inhibits dimethylnitrosamine-induced liver damage in rats. The Journal of pharmacy and pharmacology. 2003; 55:1169–1174. [PubMed: 12956909]
20. Fang R, Jing H, Chai Z, Zhao G, Stoll S, Ren F, et al. Design and characterization of protein-quercetin bioactive nanoparticles. Journal of Nanobiotechnology. 2011; 9:19. [PubMed: 21586116]
21. Gugler R, Leschik M, Dengler HJ. Disposition of quercetin in man after single oral and intravenous doses. Eur J Clin Pharmacol. 1975; 9:229–234. [PubMed: 1233267]
22. Anand P, Kunnumakkara AB, Newman RA, Aggarwal BB. Bioavailability of Curcumin: Problems and Promises. Molecular Pharmaceutics. 2007; 4:807–818. [PubMed: 17999464]
23. Lamson DW, Brignall MS. Antioxidants and cancer, part 3: quercetin. Alternative medicine review : a journal of clinical therapeutic. 2000; 5:196–208. [PubMed: 10869101]
24. Hollman PC, Gaag vd M, Mengelers MJ, van Trijp JM, de Vries JH, Katan MB. Absorption and disposition kinetics of the dietary antioxidant quercetin in man. Free Radic Biol Med. 1996; 21:703–707. [PubMed: 8891673]
25. Wilczewska AZ, Niemirowicz K, Markiewicz KH, Car H. Nanoparticles as drug delivery systems. Pharmacol Rep. 2012; 64:1020–1037. [PubMed: 23238461]
26. Jain AK, Thanki K, Jain S. Co-encapsulation of Tamoxifen and Quercetin in Polymeric Nanoparticles: Implications on Oral Bioavailability, Antitumor Efficacy, and Drug-Induced Toxicity. Molecular Pharmaceutics. 2013; 10:3459–3474. [PubMed: 23927416]
27. Wattamwar PP, Mo Y, Wan R, Palli R, Zhang Q, Dziubla TD. Antioxidant Activity of Degradable Polymer Poly(trolox ester) to Suppress Oxidative Stress Injury in the Cells. Advanced Functional Materials. 2010; 20:147–154.
28. Brey DM, Ifkovits JL, Mozia Rl, Katz JS, Burdick JA. Controlling poly(p-amino ester) network properties through macromer branching. Acta biomaterialia. 2008; 4:207–217. [PubMed: 18033746]
29. Lynn DM, Langer R. Degradable Poly(p-amino esters): Synthesis, Characterization, and Self-Assembly with Plasmid DNA. Journal of the American Chemical Society. 2000; 122:10761–10768.
30. Bose S, Michniak-Kohn B. Preparation and characterization of lipid based nanosystems for topical delivery of quercetin. European Journal of Pharmaceutical Sciences. 2013; 48:442–452. [PubMed: 23246734]

31. Wattamwar PP, Biswal D, Cochran DB, Lyvers AC, Eitel RE, Anderson KW, et al. Synthesis and characterization of poly(antioxidant beta-amino esters) for controlled release of polyphenol antioxidants. Acta biomaterialia. 2012; 8:2529–2537. [PubMed: 22426289]
32. Ritger PL, Peppas NA. A simple equation for description of solute release I Fickian and non-fickian release from non-swellable devices in the form of slabs, spheres, cylinders or discs. Journal of Controlled Release. 1987; 5:23–36.
33. Lao LL, Peppas NA, Boey FYC, Venkatraman SS. Modeling of drug release from bulk-degrading polymers. International Journal of Pharmaceutics. 2011; 418:28–41. [PubMed: 21182912]
34. Simone E, Dziubla T, Shuvaev V, Muzykantov VR. Synthesis and characterization of polymer nanocarriers for the targeted delivery of therapeutic enzymes. Methods in molecular biology (Clifton, NJ). 2010; 610:145–164.
35. Steinberg D, Witztum JL. Is the Oxidative Modification Hypothesis Relevant to Human Atherosclerosis?: Do the Antioxidant Trials Conducted to Date Refute the Hypothesis? Circulation. 2002; 105:2107–2111. [PubMed: 11980692]
36. Kerksick C, Willoughby D. The antioxidant role of glutathione and N-acetyl-cysteine supplements and exercise-induced oxidative stress. Journal of the International Society of Sports Nutrition. 2005; 2:38–44. [PubMed: 18500954]
37. Holdiness MR. Clinical pharmacokinetics of N-acetylcysteine. Clinical pharmacokinetics. 1991; 20:123–134. [PubMed: 2029805]
38. Elms A, Owen K, Albertson T, Sutter M. Fatal myocardial infarction associated with intravenous N-acetylcysteine error. International Journal of Emergency Medicine. 2011; 4:54. [PubMed: 21878099]
39. McBath RA, Shipp DA. Swelling and degradation of hydrogels synthesized with degradable poly([small beta]-amino ester) crosslinkers. Polymer Chemistry. 2010; 1:860–865.
40. Meenach SA, Otu CG, Anderson KW, Hilt JZ. Controlled synergistic delivery of paclitaxel and heat from poly(beta-amino ester)/iron oxide-based hydrogel nanocomposites. Int J Pharm. 2012; 427:177–184. [PubMed: 22326297]
41. Zhou A, Sadik OA. Comparative analysis of quercetin oxidation by electrochemical, enzymatic, autoxidation, and free radical generation techniques: a mechanistic study. J Agric Food Chem. 2008; 56:12081–12091. [PubMed: 19053369]

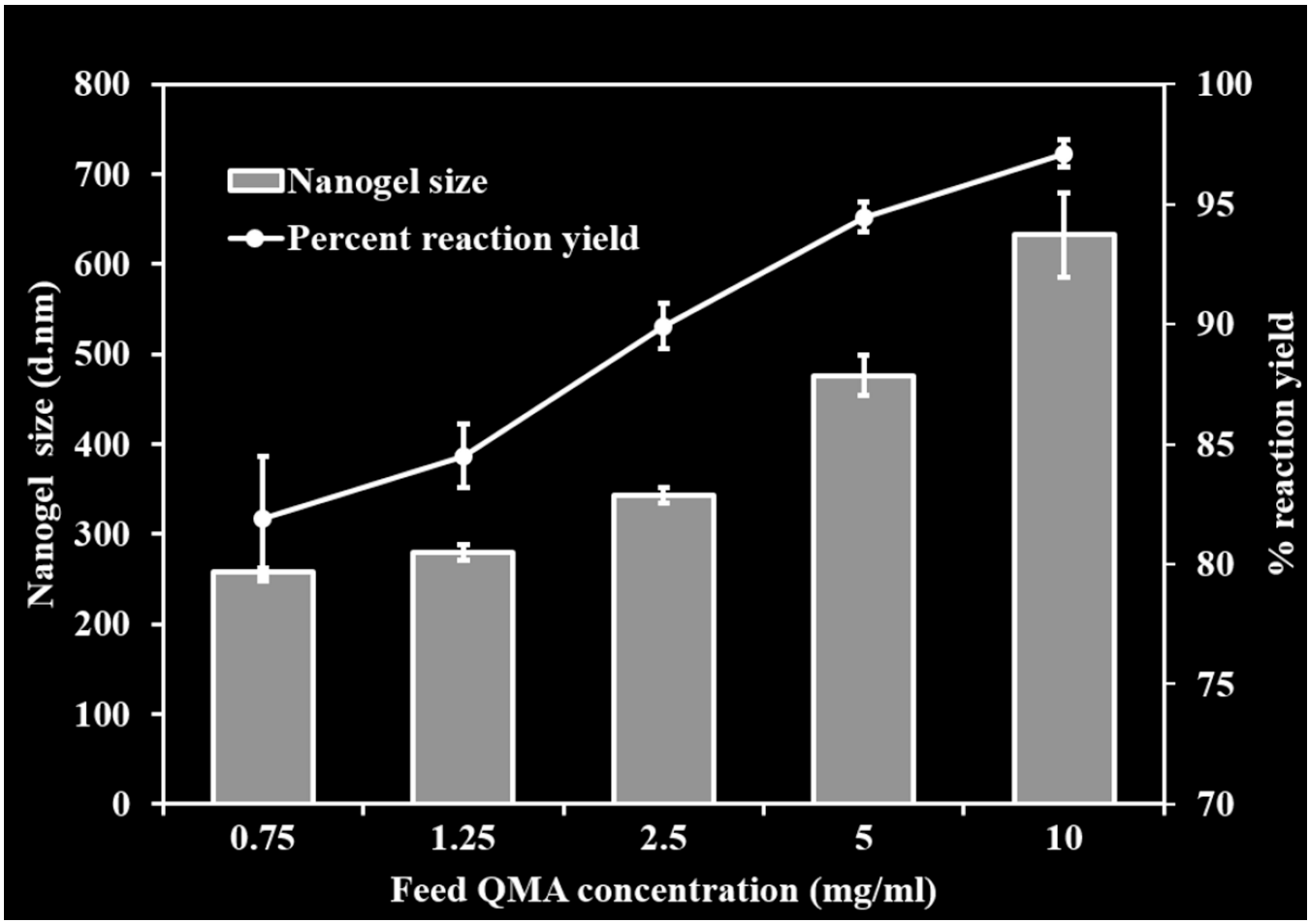

Figure 1.
Percent reaction yields and size variation of Q-PBAE nanogels with respect to variable reactant QMA concentration. (n=3, M±SD).

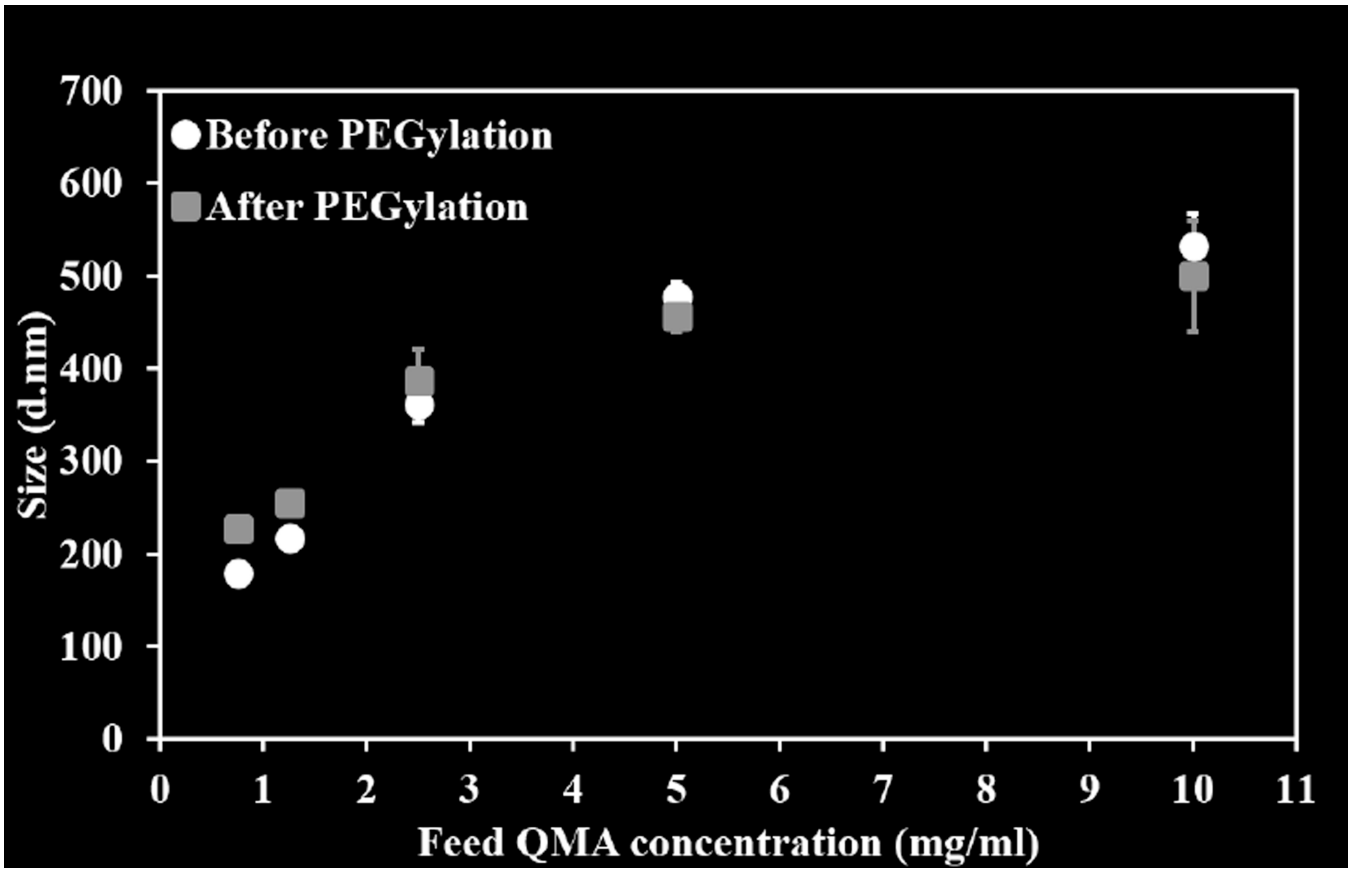

Figure 2.

Q-PBAE nanogels size variation before and after reaction with PEGMEMA4000 for 1 hour with respect to variable reactant QMA concentration measures using Dynamic light scattering in acetonitrile as suspension medium. Black circles: Nanogels diameter before reaction with PEGMEMA4000. Grey squares: Nanogels diameter after reaction with PEGMEMA4000. (n=3, M±SD)

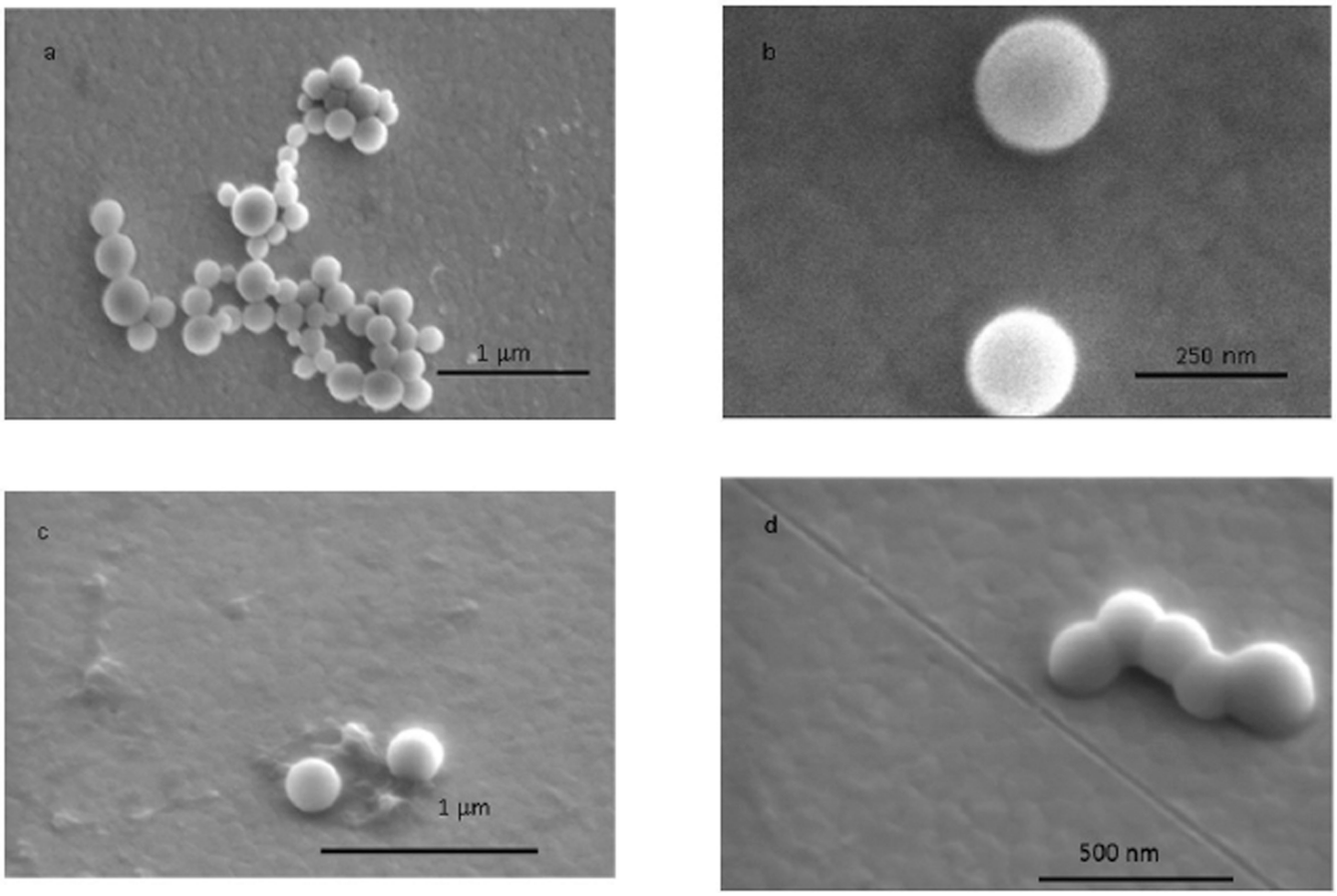

Figure 3.

Scanning electron microscopy of the Q-PBAE nanogels synthesized with reactant QMA concentration of 2.5mg/ml. a, b: plain view (Top view); c, d: angled view, 38°.

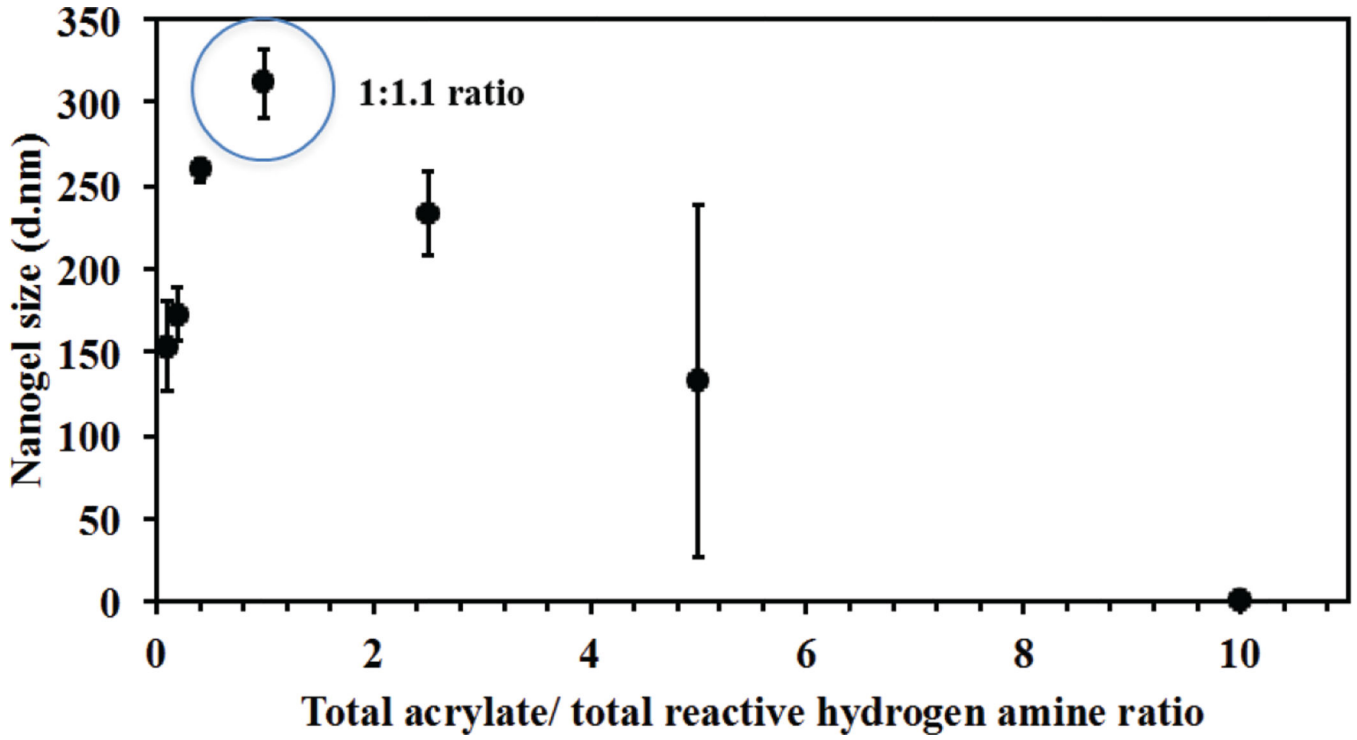

Figure 4.

Effect of total acrylate to total reactive amine hydrogen on Q-PBAE nanogels size. Variable acrylate to amine ratio ranging from 0.1 to 10 was taken and size was measured after 1 hour of reaction with 2.5mg/ml of reactant QMA concentration constant for all formulation changing the amount of amine added. (n=3, M±SD) Nanogel diameter at acrylate to amine ratio of 1.1 was found to be the highest with respect to other stoichiometric ratios mostly due to maximum extent of reaction. Hence this ratio was used for all the formulations with variable feed reactant concentrations.

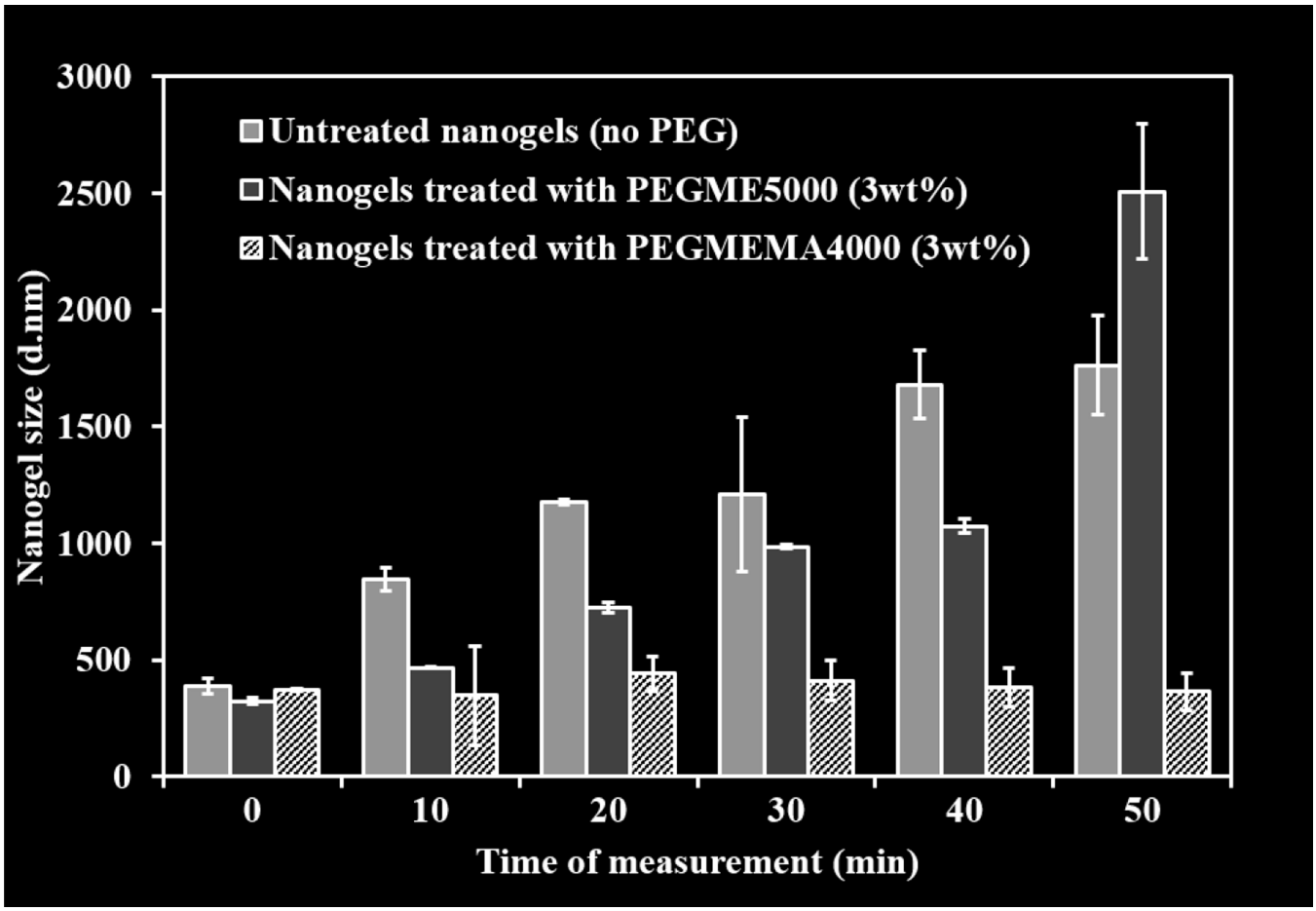

Figure 5.

Stability analysis of Q-PBAE nanogels before and after reaction with PEGMEMA4000 in PBS. Size measurements were taken at various time intervals after suspension of nanogels in PBS. Nanogels after PEGMEMA4000 coating were more stable than non-coated nanogels. Nanogels were prepared with 2.5mg/ml reactant QMA concentration and reacted with 3wt/vol% PEGMEMA4000. (n=3, M±SD)

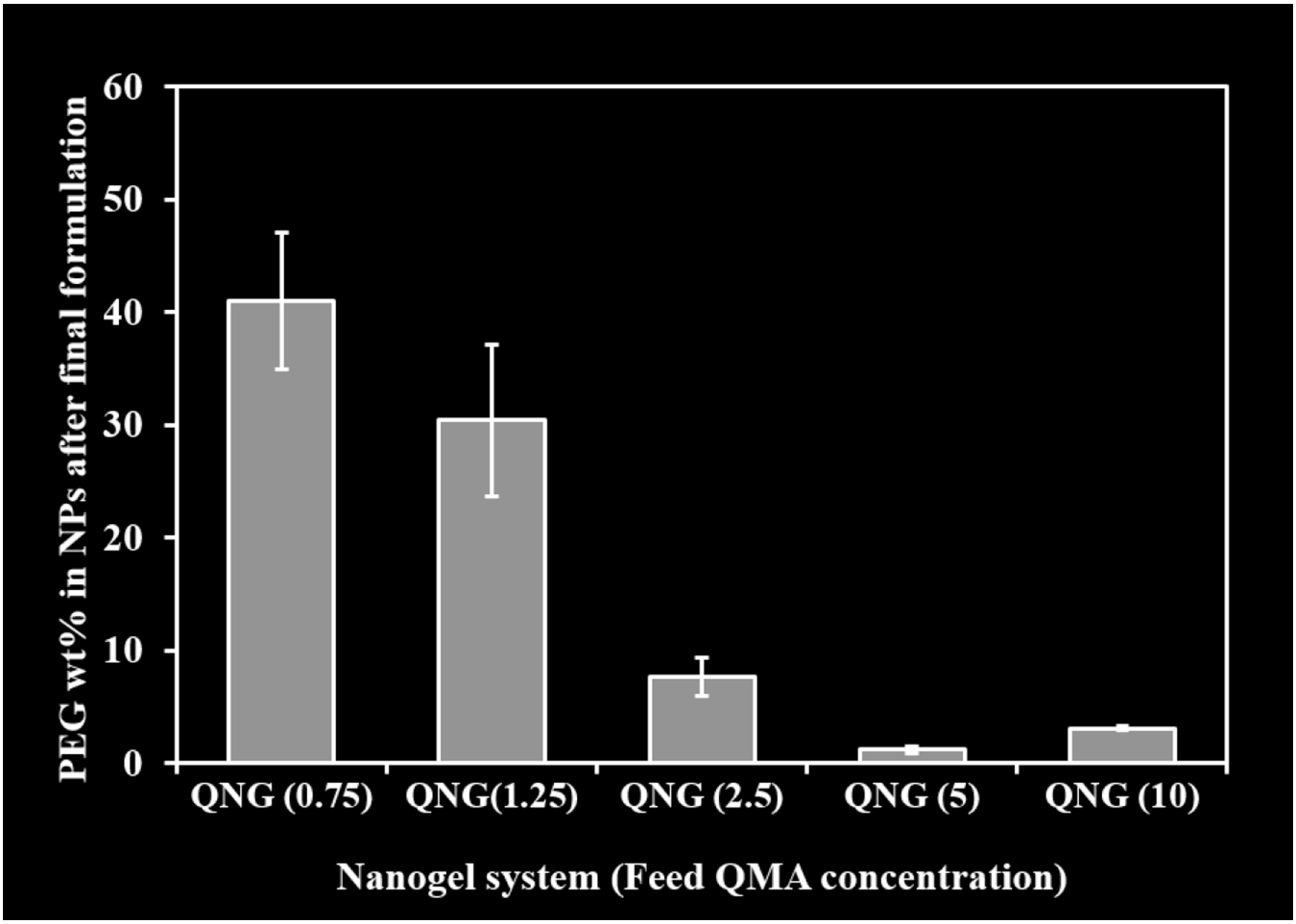

Figure 6.

PEG weight percent after the purification of nanogels with respect to variable reactant QMA concentration followed by reaction with 3wt/vol% PEGMEMA4000. Barium Iodide assay was used to determine PEG content. (n=3, M±SD)

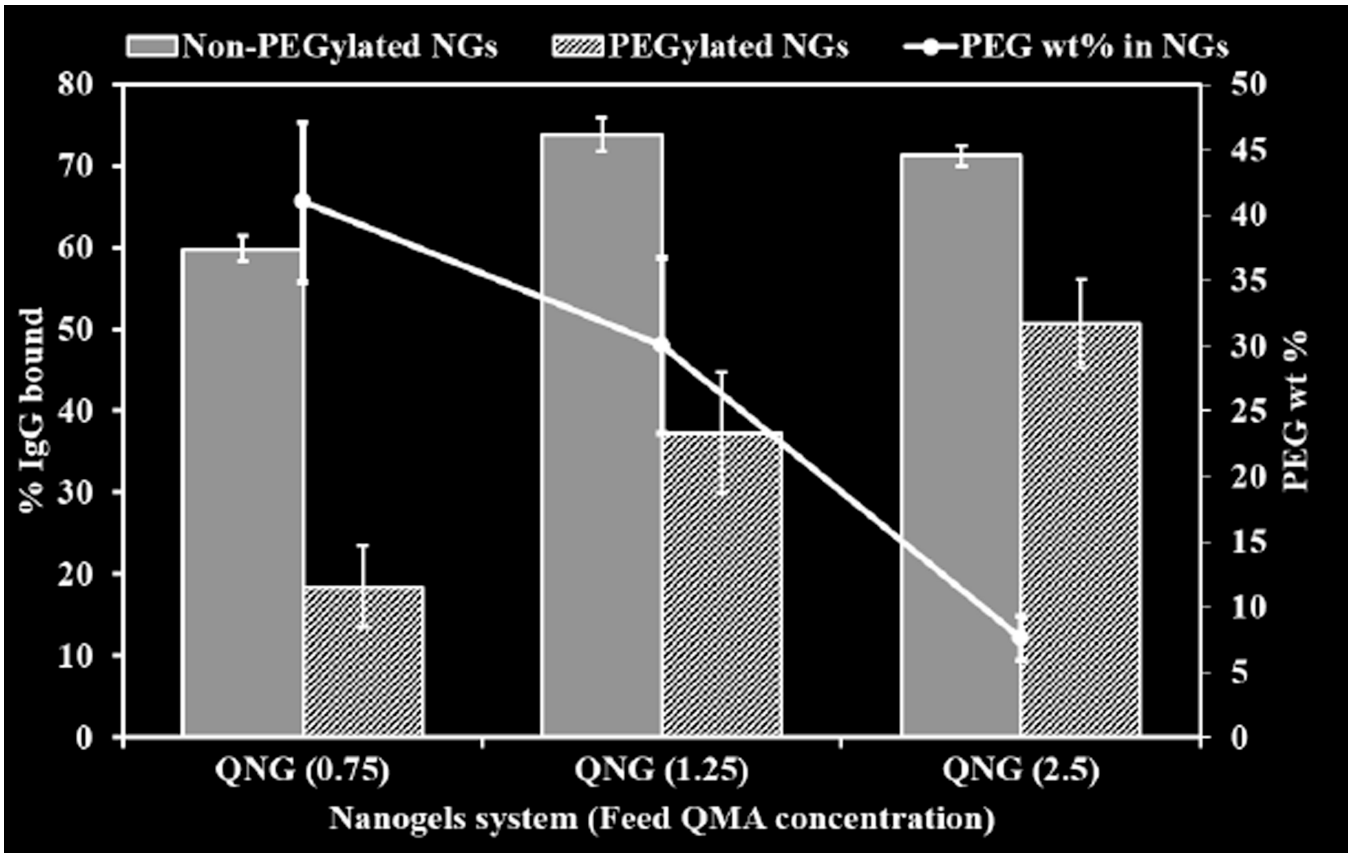

Figure 7.

Extent of IgG binding to non-PEG coated and PEG coated Q-PBAE nanogels compared in three different nanogel systems having different PEG wt% in them. (n=3, M±SD)

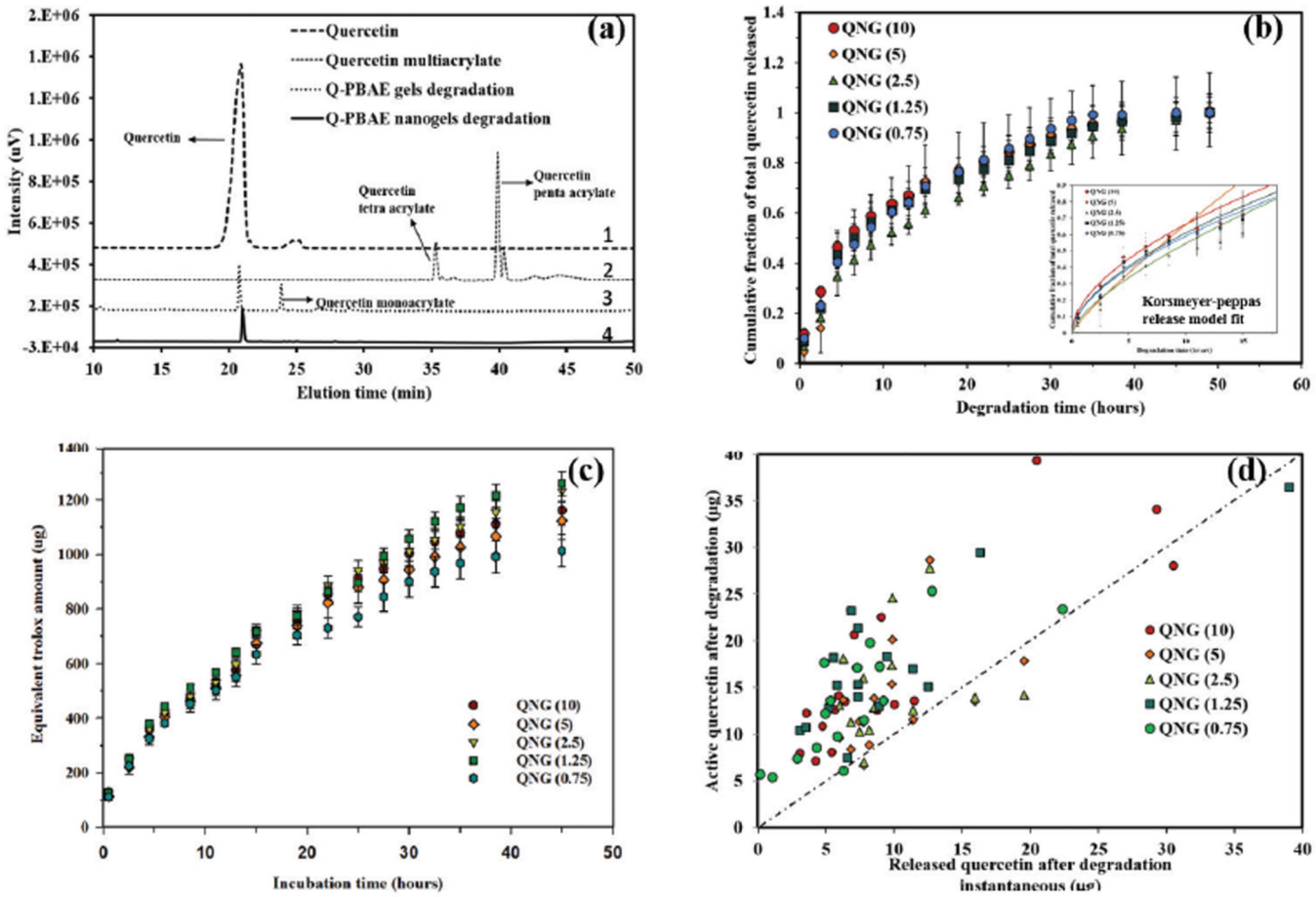

Figure 8.

(a) HPLC analysis of nanogels degradation products to confirm the recovery of pure quercetin and not any other mono or higher quercetin acrylates. This was confirmed by comparing the nanogel degradation products with quercetin, QMA (monomer) and degradation products of bulk Q-PBAE gels which results in quercetin and quercetin monoacrylate release, (b) Degradation/quercetin release profile from Q-PBAE nanogels in PBS (pH 7.4 with 2vol% DMSO). 90% of the quercetin was released within 35 hours of incubation. N=3 and the profile fits Korsmeyer-Peppas release kinetic model $\mathbf{M_t/M_{inf} = Kt^n}$ with n values within 0.45–0.85 showing anomalous release. R-square ranged from 0.9737 to 0.9923, (c) Antioxidant activity profile of the degraded products of Q-PBAE nanogels. The study was done using the trolox equivalent antioxidant capacity assay (TEAC), and the activity is expressed in terms of equivalent amount of trolox. (n=3, M±SD) (d) Instantaneous active quercetin values calculated from TEAC values compared with instantaneous quercetin released values obtained after each degradation time interval.

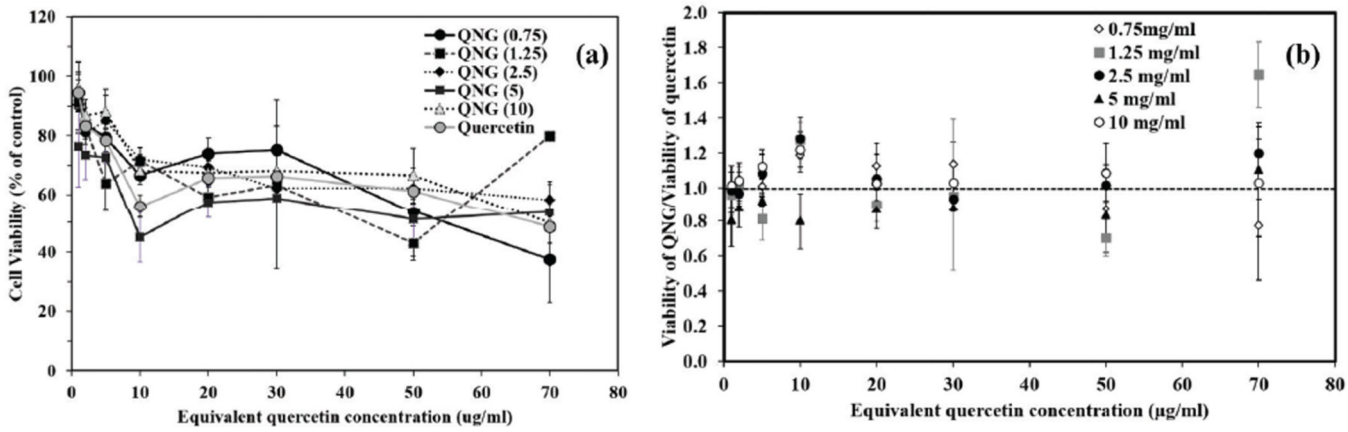

Figure 9.

(a) Concentration dependent cell viability study after exposure of HUVECs with QNGs and pure quercetin for 24 hours. Calcein AM red-orange was used as live cell tracer. (n=4, M ±SD), (b) Specific viability of QNGs with respect to quercetin. A two-way ANOVA test was conducted taking nanogel compositions and treatment concentrations as two variables. No significant difference in viability was observed due to different compositions and pure quercetin while treatment concentrations showed statistically significant difference in cell viability. (n=4, M±SE)

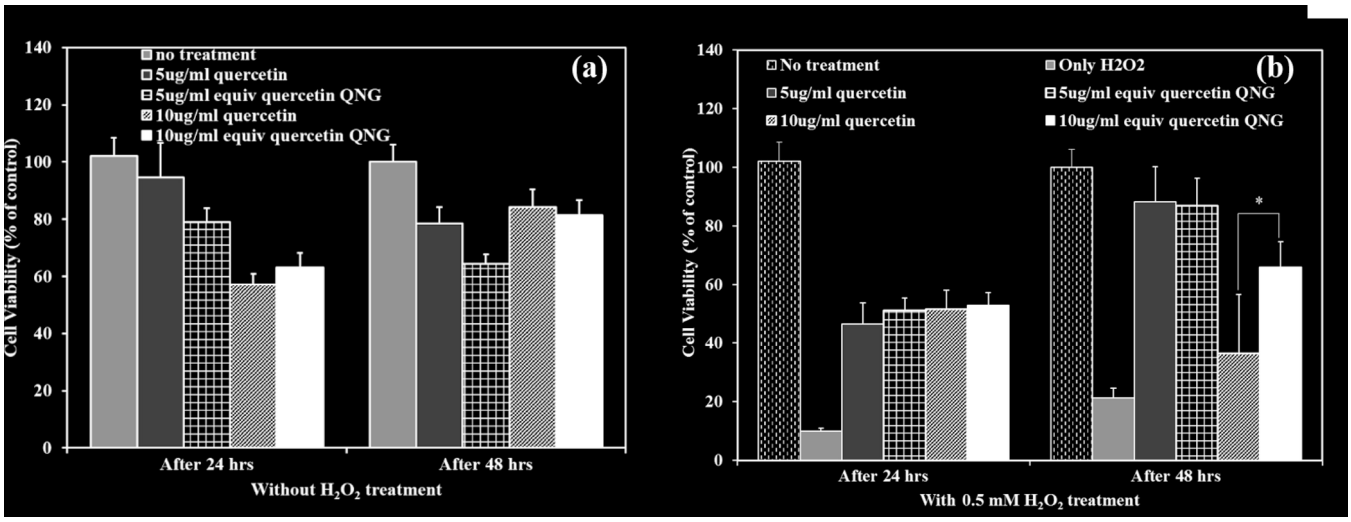

Figure 10.

Cell viability studies of HUVECs treated with two different concentrations of QNG (1.25) system: 5 and 10 μg/ml and/or 0.5mM H_2O_2. Cell death analyzed after 24 and 48 hours of treatment. (a) Treatment with only QNG/quercetin. (b) Treatment with QNG/quercetin and H_2O_2. * $p<0.05$, (n=4, M±SD)

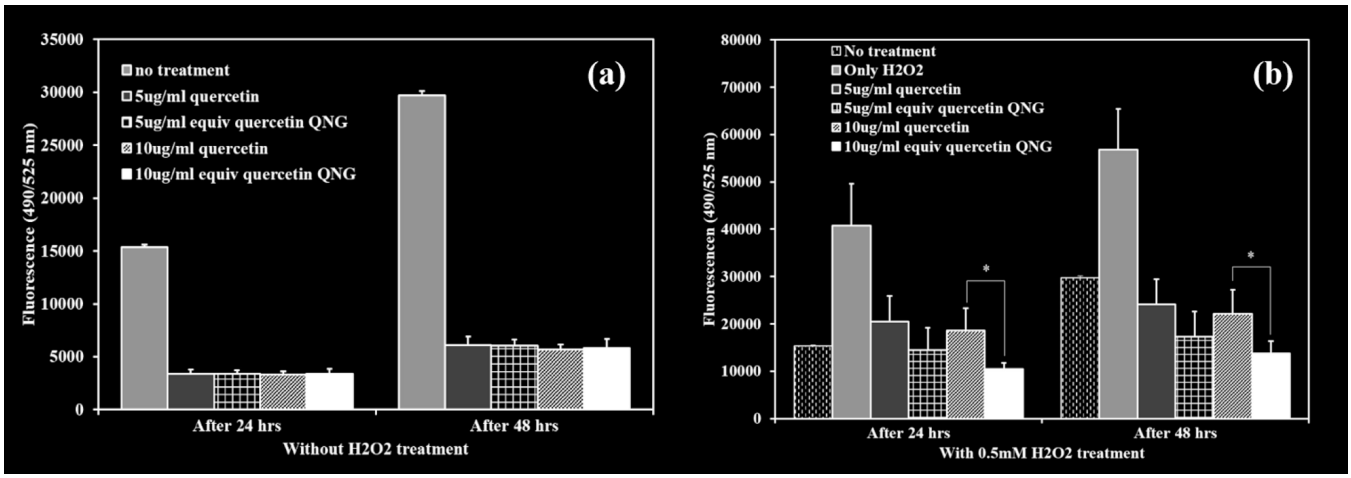

Figure 11.

Oxidative stress suppression analysis using 10 μM DCF-DA as an oxidative stress marker. Two different of QNG/quercetin, 5 and 10 μg/ml were used. Fluorescence was measured after 24 and 48 hours of treatment. (a) Treatment with QNG/quercetin. (b) Treatment with QNG/quercetin and 0.5mM H_2O_2. * $p<0.05$, (n=4, M±SD)

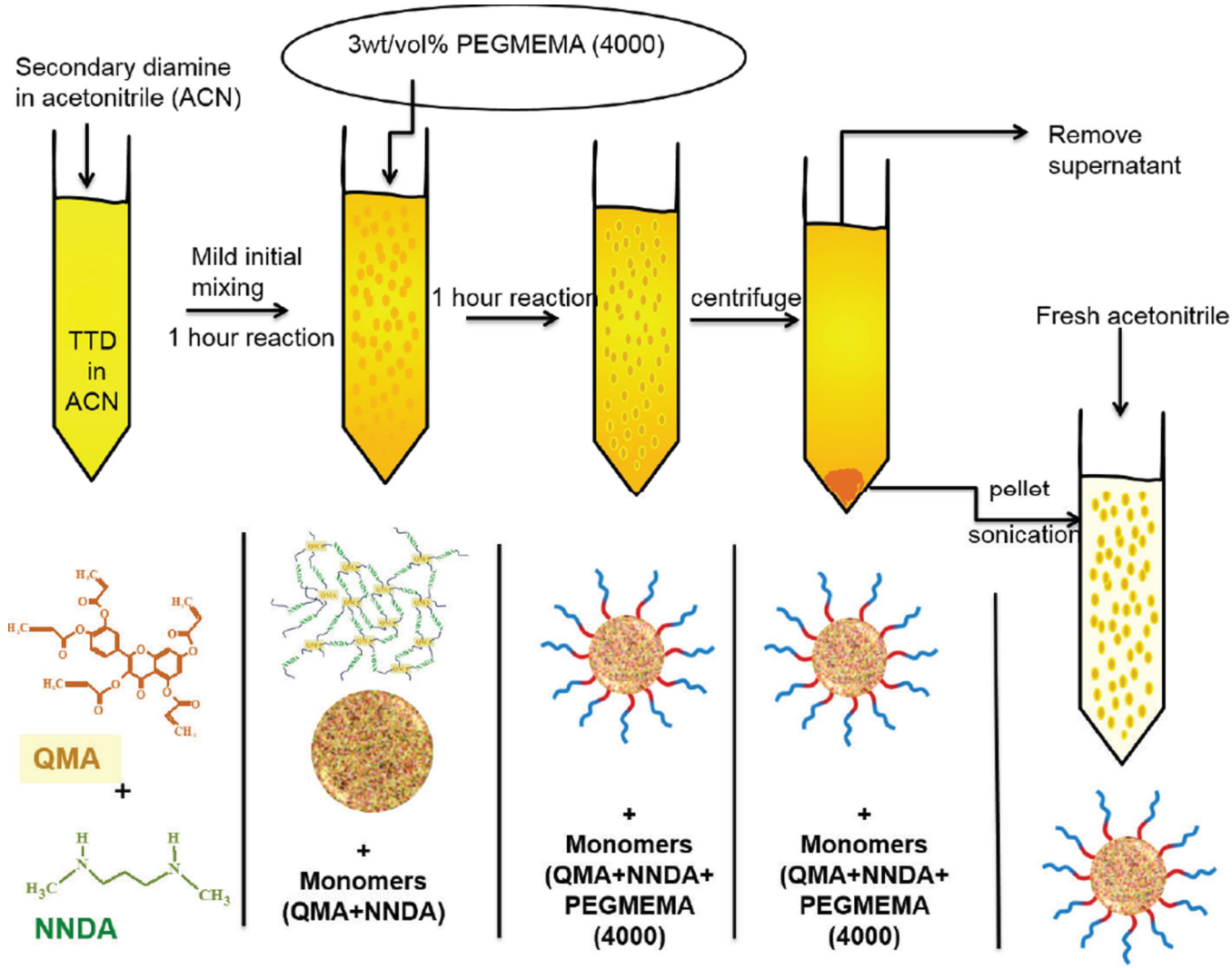

Schematic 1.
Schematic of Q-PBAE nanogels synthesis